Proceedings of the Sixth International Conference on
Railway Technology: Research, Development and Maintenance
Edited by: J. Pombo
Civil-Comp Conferences, Volume 7, Paper 5.10
Civil-Comp Press, Edinburgh, United Kingdom, 2024
ISSN: 2753-3239, doi: 10.4203/ccc.7.5.10

Study on the Mechanism of Wheelset Angular Velocity Changing on Curved Tracks

Y. Endo[1], Y. Michitsuji[2], M. Tanimoto[3] and O. Imahori[4]

[1] Graduate School of Science and Engineering, Ibaraki University Hitachi, Japan
[2] College of Engineering, Ibaraki University Hitachi, Japan
[3] Engineering Department, Metro Sharyo Co., Ltd. Tokyo, Japan
[4] Rolling Stock Department, Tokyo Metro Co., Ltd. Tokyo, Japan

Abstract

The change of wheelsets' rotation angular velocity on curved tracks introduces velocity estimation errors, leading to inaccuracies in train positioning for the moving block system utilized by communication-based train control. Therefore, elucidating the mechanism and characteristics of angular velocity changing is crucial for assessing the accuracy of train location estimation. In this study, experiments and multi-body dynamics simulations were conducted to observe angular velocity changes on curved tracks. The experimental results indicates the changes of angular velocity on curved tracks, with the rotation of the front axle of the bogie notably slower than that of the rear axle. Simulation results indicate that the observed physical phenomenon can be replicated, with the relative change in angular velocity differing based on wheel/rail friction coefficient conditions. The mechanism of this variation is discussed in terms of path length differences between wheels, changes in rolling radius, and longitudinal creepages. Consequently, it is concluded that the distinct characteristics of longitudinal creepage depending on conditions are the primary determinant of the differential angular velocity of wheelsets on curved tracks.

Keywords: communication-based train control, moving block system, velocity measurement, angular velocity of wheelset, train localization, steering bogie

1 Introduction

The block system is the basic principle of the train signaling. To maintain a safe separation between trains, This system defines the sections called blocks which only one train is allowed at a time. As one kind of the block system, the fixed block system is used conventionally. It devides a railway track into blocks, and detect whether the train is in blocks by the track circuit. This system is regarded as the reliable system and be diffused globaly. However, this system have some challanges in view of efficient train operation and management. For example, there is wasted occupied areas because the track circuit cannot estimate the detailed train locations in the block system. Furthermore, the system needs a lot of electrical facilities on ground which needs to be maintained such as the signal lights and the relay system for the track circuit.

In recent years, the moving block system, facilitated by the CBTC (Communication-Based Train Control) system, has garnered attention as more efficient train control system than the fixed block system. It establishes an occupied block with safety margins for each train, dynamically and continuously moving with the trains, commonly called the "moving block". The placement of the moving block relies on the real-time train location information transmitted from each train. This dynamic control of blocks enables more efficient use of railway capacity, which contributes more frequent train oparation while maintaining safety. It can also achieve the reduction of trackside facilities which need to be maintained because the facilities for the track circuits and signal lights are no longer needed[1].

To introduce this system, it is necessary to establish a method to detect accurate train locations by the onboard system. One of the methods is to calculate based on the rotation of the wheelset. The train location can be represent by the traveling distance from the reference point. The traveling distance of the train can be calculated by integrating the estimated translational velocity which calculated by multiplying the angular velocity of wheelset and nominal wheel radius. However, the angular velocity of the wheelset can be different between the axles on straight and curved sections on the tracks even the same translational velocity, It can be introduced by the specific behaviors of the wheelset on curved tracks, such as wheel/rail contact point changing and longitudinal creepages. This phenomenon causes the velocity measurement error which leads to the error in train location estimation. Therefore, there is a possibility that the rotation behavior of wheelset affects the accuracy of train location estimation which is important for the safety and efficiency of the moving block system.

This study explores the dynamics of wheelset angular velocity changes in view of vehicle dynamics. Experimentals and multi-body dynamics (MBD) simulations are conducted to evaluate angular velocity changings on curved tracks. Furthermore, the simulation investigates how the angular velocity change is affected by an asymmetric wheel/rail friction coefficient condition, particularly stemming from high rail lubrication. Additionally, factors contributing to these changes are identified and quantified as "influence rates" for each conditions. Drawing on these findings and discussions, differences in the mechanisms of wheelset angular velocity changes on curved tracks are analyzed by conditions. This analysis is facilitated through visualization methods applied to the formulated influence rates.

2 Methods

2.1 Conditions of experiments and simulations

To evaluate the angular velocity changes of the wheelset in curved tracks, experiments with railway vehicles were conducted. In this evaluation, the angular velocity of the axles on both the straight and curved sections of the track at the same translational velocity is compared. Additionally, a MBD simulation was conducted under identical conditions. The purpose of it is to verify whether the rotational behavior of the wheelset can be accurately reproduced through numerical simulation. Furthermore, simulations under the condition supposing to the high rail lubrication are also conducted to evaluate the effect of asymmetric wheel/rail friction coefficient conditions on the angular velocity changes.

For the evaluation, railway vehicles designed for subway lines were utilized as test vehicles. The vehicles consisted of a six-car train, equipped with sensors installed on both end cars to measure the rotation of wheelsets on the second and third axles. Additionally, these vehicles were equipped with single-axle steering bogies. The mechanism and effects of the bogie are illustrated in Figure 1. The bogie steers the second and third axles, with the steering devices moving in relation to the relative yaw angle between the bolster and bogie frame. This mechanism contributes to reducing the angle of attack for the front axle of the bogie and enlarging the rolling radius difference for the rear axle of the bogie, thereby improving the curve negotiation performance for the bogie[2].

The method of experiments are shown in Figure 2. In the experiments, the rotations of the second and third axles are measured; their outcomes are represents characteristics of the rear and front axles of the bogie, respectively. The first and last cars of the train were initially brought to a stop within curved and straight sections of the track, respectively. Starting from the moment the vehicle began to move, rotation angle measurements were initiated for the axles for evaluation. The vehicle was then accelerated to approximately 10 km/h, followed by maintaining a constant speed. Subsequently, the vehicle decelerated, and rotation angle measurements were stopped upon coming to a complete stop. The traveling distance of the experiments are about 90 m. The measured rotation angles of axles traveled on the curved and straight sections are represented by θ_c and θ_s, respectively. The change in rotation angles is evaluated by the relative change of θ_c to θ_s; its value is represented by ε_θ. To focus on the angular velocity changing during curve passage, the effects of slip or skid should be eliminated. Therefore, brake and traction forces were not applied to the measurement axles. The experiments were conducted on the track in the rail yard, which includes a curved section with a radius of 169 m. The track gauge is 1435 mm, and there are no superel-

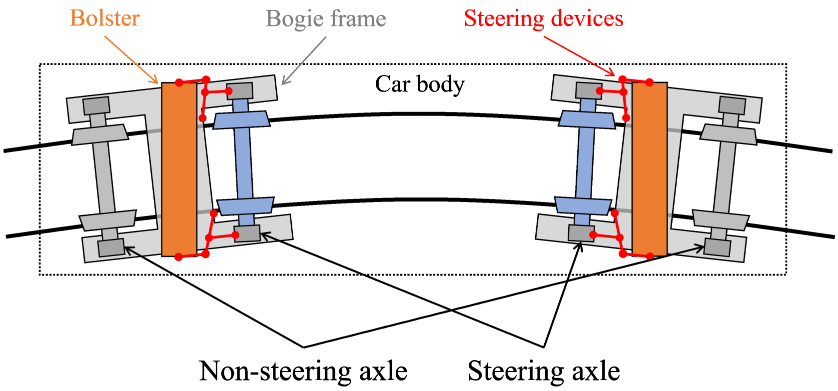

Figure 1: Mechanism of single-axle steering bogie. The bogie steers second and third axles by the steering devices moving in relation to the relative yaw angle.

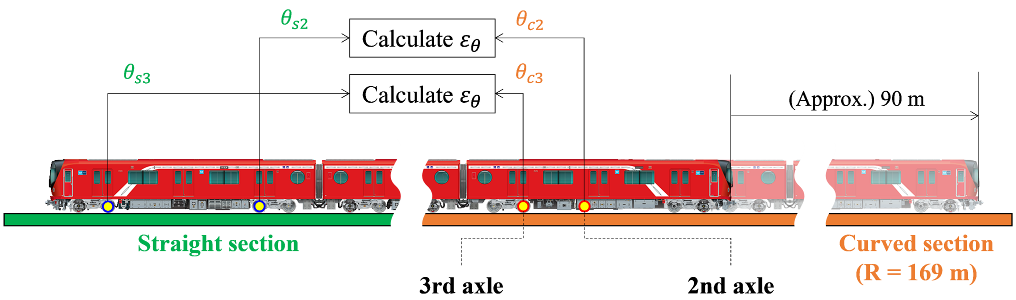

Figure 2: Method of experiments. Relative change in rotation angle of wheelset is evaluated by comparing between measured rotation angles of axles travels on curved and straight sections.

evations and slacks. Notably, the rails on the track were not lubricated, resulting in an anticipated wheel/rail friction coefficients of approximately 0.3 on both sides.

The simulations were conducted by utilizing the MBD simulation software, Simpack Rail. Here, the FASTSIM is employed as a wheel/rail contact algorithm. The simulation conditions are basically matched to those of the experiments. The railway vehicle model, as shown in Figure 3, accurately represents the specifications of the test vehicles, including the mechanism of the single-axle steering bogie. The geometrical layout of the track were also equal to the experiments. The wheel/rail friction coefficient (μ) condition is set to 0.3 as a basal condition. The comparison with the experiments is evaluated based on this condition. In addition to comparing with the experiments, the study evaluates the effect of an asymmetric friction coefficient condition, assuming high rail lubrication. In that condition, the friction coefficient on the high rail (μ_{out}) is set to 0.1, while that on the low rail (μ_{in}) remains at 0.3 as par the basal condition. The difference of the angular velocity at 10 km/h is also evaluated in the simulations in addition to that of the rotation angle; the angular velocity of

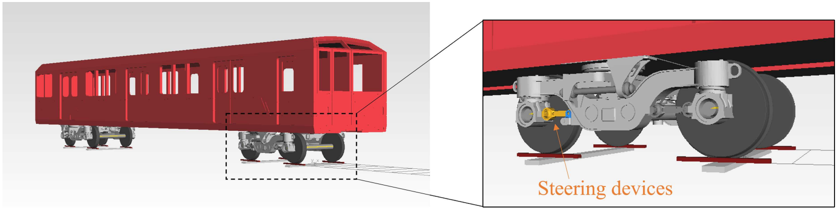

Figure 3: MBD simulation model. The specifications of the test vehicle, including the mechanism of the single-axle steering bogie, are accurately represented.

axles traveling curved and straight sections are represented by ω_c and ω_s, respectively. Likewise ε_θ, the relative change in ω_c to ω_s is represented by ε_ω. Notably, if ε_ω has no velocity dependence, the value of it is the same as the ε_θ.

3 Results and discussions

Figure 4 presents calculated ε_θ values derived from the observed angular velocities in the experiments. The vertical length of points indicates the range of error in the rotation angle caused by sensor resolution. As depicted in the figure, the rotation angle of axle traveling the curved section differs from that traveling the straight section. This implies a changing in the angular velocity of axles between curved and straight sections. Additionally, a clear correlation between ε_θ and the axle position in the bogie is observed. The ε_θ values of the front axle exhibit larger negative values cmpared to those of the rear axle, indicating that the angular velocity of the front axle during curved sections is slower than that of the rear axle.

Figure 5 depicts the outcomes of the MBD simulation conducted under the basal friction coefficient condition. The values of ε_θ and ε_ω are illustrated in Figure 5(a) and Figure 5(b), respectively. In Figure 5(a), a similar trend in ε_θ to that observed in the experiment is evident. The values of ε_θ closely align with the experimental data, and the relationship between the front and rear axles of the bogie regarding ε_θ mirrors that observed in the experiments. These consequences suggest that the physical phenomenon of the angular velocity changing can be simulated by the MBD simulation with FASTSIM algorithm. Additionally, these results suggest that ε_θ can effectively serve as a representative measure for ε_ω, as their values are nearly identical for both axles. This indicates negligible velocity dependence for ε_ω.

Figure 6 indicates the comparison between the simulation results with basal and asymmetric wheel/rail friction coefficient conditions. The figure shows that ε_ω are changed depending on the friction coefficient conditions; them of the front and rear axles becomes more positive and negative, respectively.

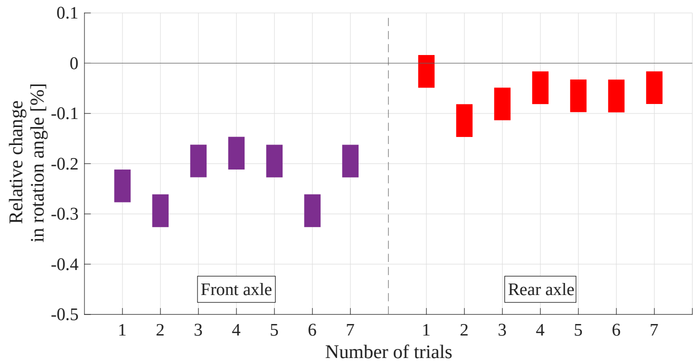

Figure 4: Experimental results about the relative change in rotation angle of wheelsets.

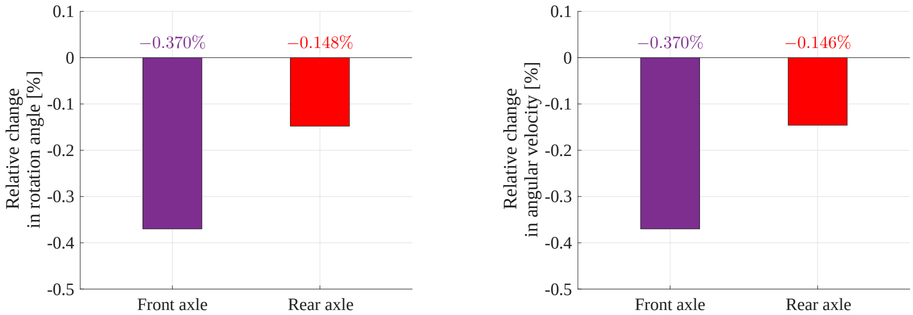

(a) Rotation angle (b) Angular velocity

Figure 5: Simulation results about the relative change in the rotation angle and angular velocity of wheelsets.

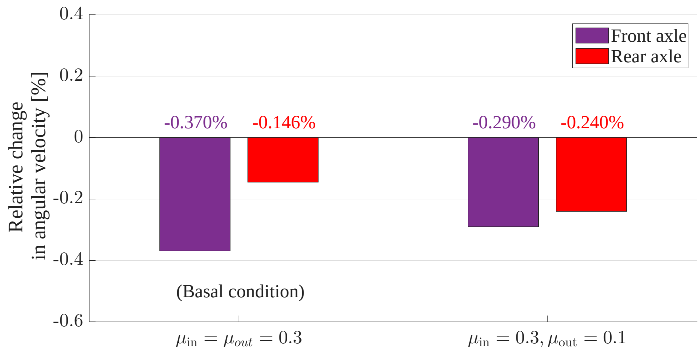

Figure 6: Simulation results about the relative change in the angular velocity of wheelsets; the comparison between the basal and asymmetric wheel/rail friction coefficient conditions.

4 The mechanism of the angular velocity changing

4.1 Formulation of the changing factors

There are three factors to explain the mechanism of the angular velocity changing on curved track; path length difference between inner and outer wheels, wheel rolling radius changing, and the longitudinal creepages[3]. Hereinafter, effects of them are discussed separately.

First, the effect of the path length difference is explained. Since the arc length of the high and low rails differ, and the wheelset rotates with straddling the rails, the dependence on the rails can be one of the factors affecting the rotation of the wheelset on curved tracks. To illustrate this effect, a basic example depicted in Figure 7(a) is considered. In this example, a wheelset with independently rotating wheels which have cylindrical treads with wheel radius of r_0 traveling a curved track with a radius of R is assumed. Here, b represents the difference between the curve radius at the track centerline and the turning radius of the wheel. The translational velocity of the wheelset based on the track centerline is denoted as v_s, while v_{in} and v_{out} represent the translational velocities of the inner and outer wheels, respectively, based on their contact points with the rails. As a reference value of rotation angular velocity, $\omega_s = v_s/r_0$ is defined. ω_s is defined, which is considered equivalent to the rotation angular velocity of wheels on a straight track. When the wheelset travels with the turning (yaw) angular velocity of $\mathit{\Omega}$, the translational velocity v of any side of the wheels with a rotation angular velocity of ω is given by:

$$v = r_0\omega = (R + b)\,\mathit{\Omega} \tag{1}$$

Consequently, the relative change in the angular velocity of the wheels, $\varepsilon_{\text{rail}}$ is expressed as follows:

$$\varepsilon_{\text{rail}} = \frac{\omega - \omega_s}{\omega_s} = \frac{r_0\omega - r_0\omega_s}{r_0\omega_s} = \frac{(R + b)\,\mathit{\Omega} - R\mathit{\Omega}}{R\mathit{\Omega}} = \frac{b}{R} \tag{2}$$

Secondly, the effect of wheel rolling radius changing is discussed. Here, the rolling radius is defined as the radius of the wheel at the wheel/rail contact point. Typically, the profile of wheels have a gradient which contributes to a self-steering characteristic of a wheelset. To navigate a curved track, the contact points on the wheels vary laterally to increase the rolling radius difference. This characteristic of the wheelset can influence its rotation. As a basic example, a sole conical wheel with the initial rolling radius of r_0 is assumed (see Figure 7(b)). When the wheel travels at translational velocity of v_s and its rolling radius changes from r_0 to r, the rotation angular velocity of the wheel changes from $\omega_s = v_s/r_0$ to $\omega = v_s/r$. In this case, the relative change in the angular velocity, denoted as $\varepsilon_{\text{wheel}}$, can be expressed as:

$$\varepsilon_{\text{wheel}} = \frac{\omega - \omega_0}{\omega_0} = \frac{v_s/r - v_s/r_0}{v_s/r_0} = \frac{r_0 - r}{r} \tag{3}$$

Lastly, the effect of the longitudinal creepage is discussed. Longitudinal creepage occurs when the peripheral velocity of a wheel at the wheel/rail contact point, denoted as v_p, differs from the translational velocity of the wheel/rail contact patch, denoted as v_c[4]. This mismatch results in micro slip in the longitudinal direction. One way to quantify the degree of longitudinal creepage, denoted as ν_x, is given by the following formula:

$$\nu_x = \frac{v_p - v_c}{v_c} \tag{4}$$

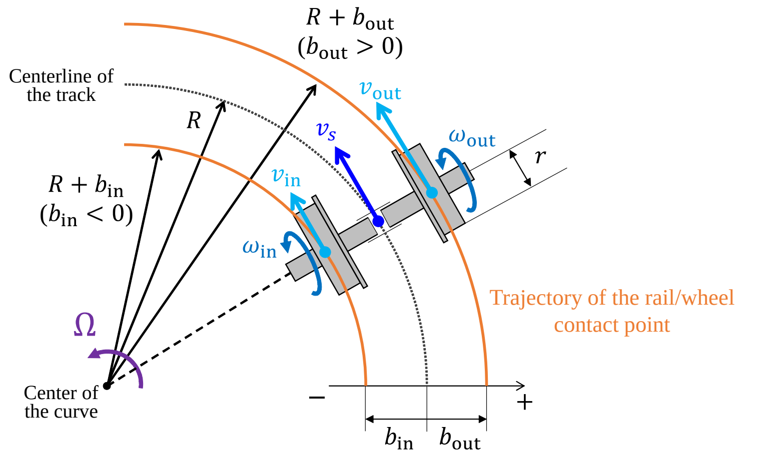

(a) About $\varepsilon_{\text{rail}}$

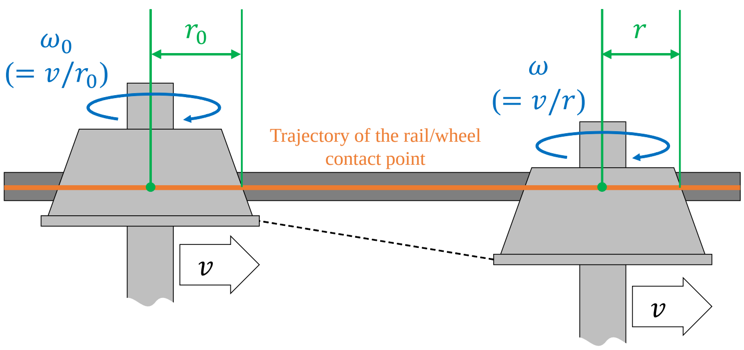

(b) About $\varepsilon_{\text{wheel}}$

Figure 7: Simple examples for mechanisms which affect to wheelset's angular velocity changing in curved tracks.

The quantities $\varepsilon_{\text{rail}}$, $\varepsilon_{\text{wheel}}$, and ν_x represent the relative change in angular velocity of the wheelset when each of these factors individually affects the angular velocity on a curved track. Here, these values are defined as the "influence rates" for angular velocity changes. If the mechanism of a wheelset's angular velocity change on a curved track can be described by these three factors, the relative change in angular velocity can be calculated by summing the influence rates as follows:

$$\varepsilon_{\omega} = \varepsilon_{\text{rail}} + \varepsilon_{\text{wheel}} + \nu_x = \frac{b}{R} + \frac{r_0 - r}{r} + \frac{v_p - v_c}{v_c} \tag{5}$$

This hypothesis is veridated using simulation results. The estimated value of ε_{ω} derived from Eq. 5 is calculated based on the simulation outputs, and compared with the true value of ε_{ω}, as illustrated in Figure 8. The figure indicates that the estimated ε_{ω} align with the true values for both axles. Therefore, the hypothesis stands true, indicating that the mechanism governing the angular velocity change of the wheelset can be described by three factors mentioned above.

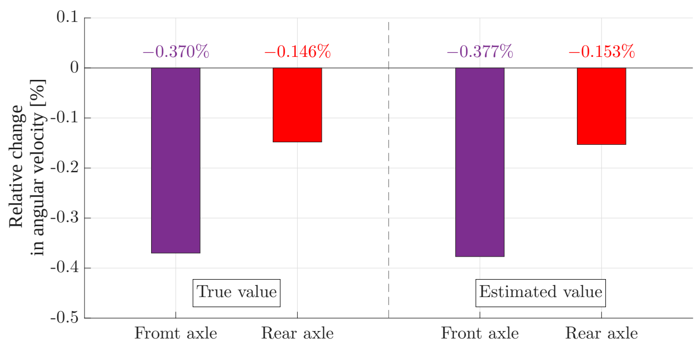

Figure 8: Comparison between the true and estimated values of ε_ω. They are almost matched, which suggests that the hypothesis about the mechanism of the angular velocity changing is true.

4.2 Visualization method for influence rates of the angular velocity changing

Now that the factors affecting the rotation of the wheelset are clarified and are formulated their influence rates, we can discuss the mechanism of angular velocity change. To facilitate this discussion, the effects of these changing factors are visualized.

Below, the method of expression by this method is elucidated with reference to the example depicted in Figure 9. In this example, a wheelset with arc wheel profiles travels a curved track with a radius of R. Notably, there is a single wheel/rail contact point on both the inner and outer wheels. For each of these contact points, the influence rates outlined in Eq.5 are assumed to be calculated. The resulting values are then visualized using colored bars, as shown in Figure10. The resulting value of ε_ω is indicated by a yellow point.

The influence rates for each parameter are explained. $\varepsilon_{\mathrm{rail}}$ values for both inner and outer wheels extend in opposite directions with nearly the same lengths, a geometrically obvious consequence considering the length relationship between the high and low rails and the track centerline. $\varepsilon_{\mathrm{wheel}}$ for both wheels extends in opposite directions relative to $\varepsilon_{\mathrm{rail}}$, representing the self-steering characteristics of a wheelset, aiming to cancel the path length difference between the inner and outer wheels by enlarging the wheel radius difference. However, the absence of intersection between the $\varepsilon_{\mathrm{wheel}}$ bars for inner and outer wheels suggests that the difference in rolling radius is not enough to compensate for the path length difference. Consequently, longitudinal creepages occur to compensate for this difference, represented by the red ν_x bars. Longitudinal creep forces act as a couple on a wheelset when no traction or brake forces are applied, causing the ν_x bars to extend in opposite directions for each wheel. Additionally, assuming that the absolute value of ν_x about the outer wheel is larger than that about the inner wheel suggests that the outer wheel is more slippery than the inner wheel, possibly due to lower friction coefficients and weaker normal forces at the contact points

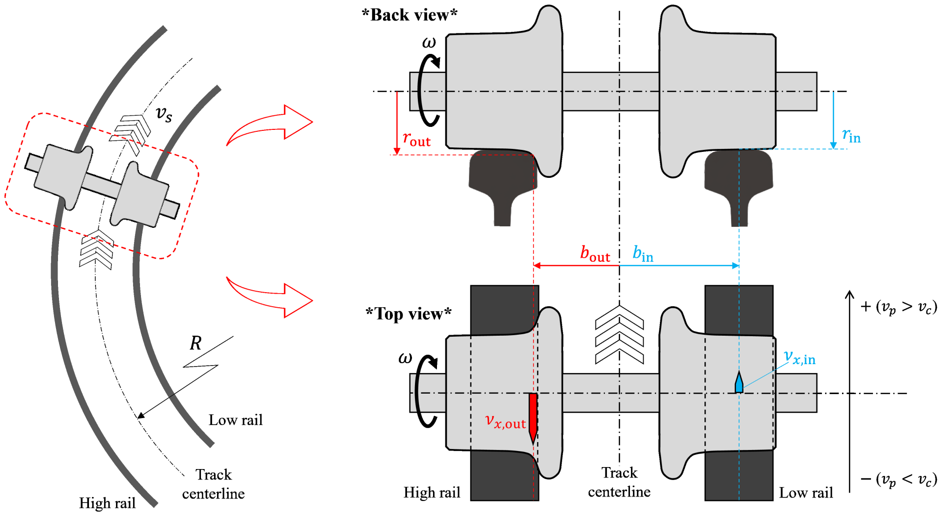

Figure 9: Example for explanation of visualization method for effects of influence rates of wheelset's angular velocity.

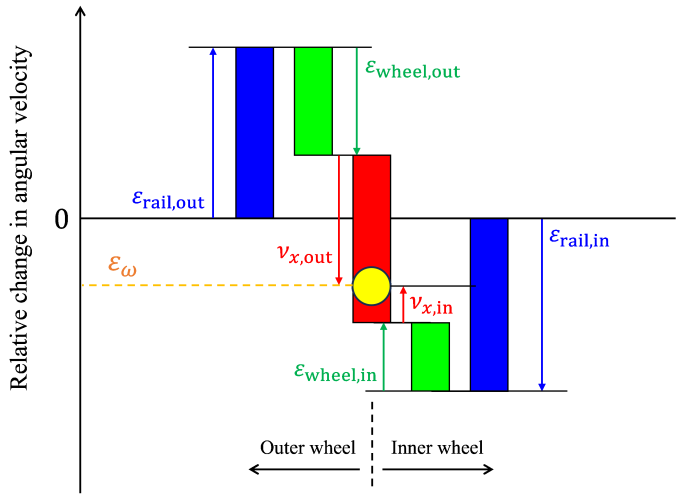

Figure 10: The example of visualization results of influence rates.

on the outer wheel.

In this way, the mechanisms of the angular velocity changes on curved tracks can be discussed more comprehensively.

4.3 Discussions for the simulation results with the visualization

By the described visualization method, the changing factors of the rotation angular velocity can be discussed. Here, only the visualization results for the inner wheels are presented because multiple-point contacts on the outer wheels are occurred in the simulations which complicates the discussion with the visualization. Figure 11 illustrates the visualization of the influence rates under the basal condition. In the figure, the directions and lengths of the $\varepsilon_{\text{rail}}$ and $\varepsilon_{\text{wheel}}$ bars are nearly identical between the front and rear axles. The $\varepsilon_{\text{rail}}$ bars extend in the negative direction with nearly the same lengths, a result consistent with the geometric relationship between the track centerline and the low rail. Positive values of $\varepsilon_{\text{wheel}}$ indicate that the rolling radii of the inner wheels are smaller than those at the neutral position. Additionally, similar $\varepsilon_{\text{wheel}}$ values suggest that the lateral positions of the wheelsets are nearly equal. Consequently, the rear axles of the bogie are laterally displaced similar to the front axle, contrary to the expectation that the rear axle of a bogie without steering mechanisms typically remains near the neutral position[6]. This outcome likely reflects the characteristics of a single-axle steering bogie aimed at increasing the rolling radius difference of the rear axle. The main difference between the front and rear axles lies in the values of ν_x. The red ν_x bars for the front and rear axles extend in opposite directions, indicating negative and positive values, respectively. Considering yaw moments generated by longitudinal creep forces, the negative and positive ν_x values on inner wheels imply steering and anti-steering moments exerted by the longitudinal creep forces, respectively[4]. This observation aligns with the well-known relationship regarding the directions of longitudinal creepages for the front and rear axles on curved tracks. Through this visualization method, it becomes evident that the primary cause of the differing angular velocity changes between the front and rear axles observed in the experiments is the distinct directions of the longitudinal creepages.

Figure 12 compares the basal and asymmetric friction coefficient conditions for the front and rear axles of the bogie. The figures suggest that the main difference between the friction coefficient conditions lies in the values of ν_x, while $\varepsilon_{\text{rail}}$ and $\varepsilon_{\text{wheel}}$ show little difference. This indicates that the lateral positions of wheelsets are less affected by the friction coefficient conditions, whereas longitudinal creepages are influenced by these conditions. In the asymmetric friction coefficient conditions, the absolute

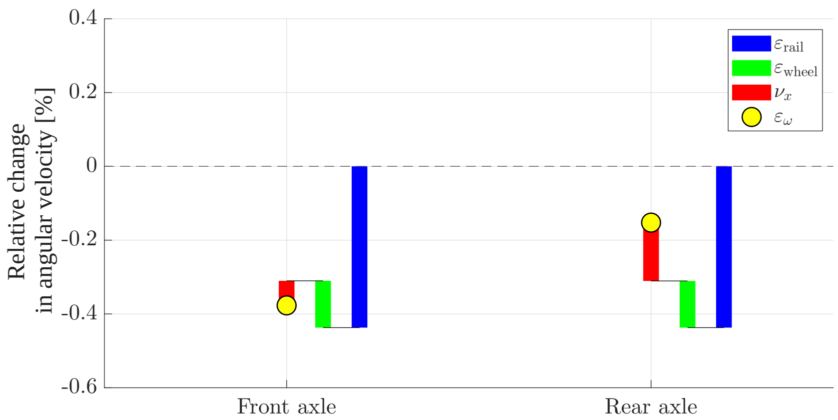

Figure 11: Visualization results of influence rates for the basal condition

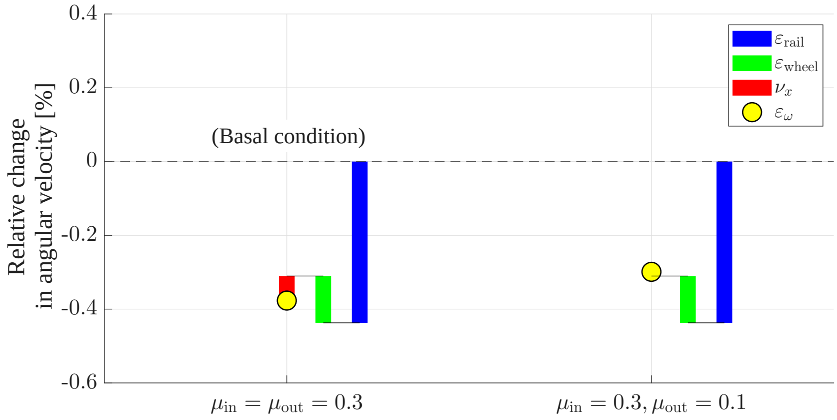

(a) Front axle

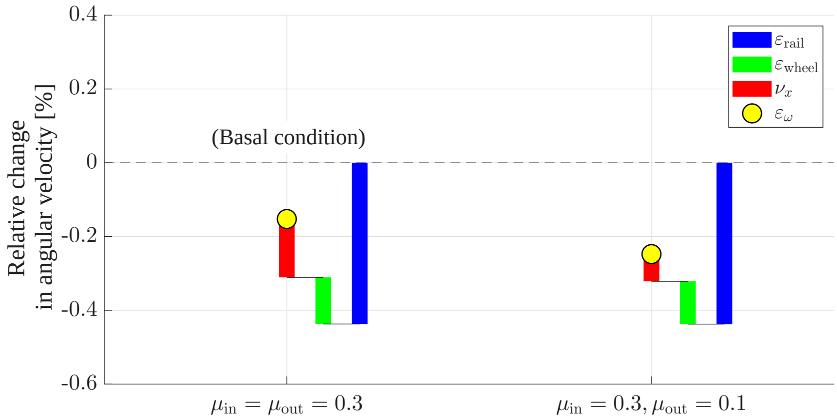

(b) Rear axle

Figure 12: Comparison of visualization results of influence rates between the basal and asymmetric wheel/rail friction coefficient conditions.

values of ν_x are smaller than those in the basal condition for both axles. This is likely due to the friction coefficient relationship between the high and low rails, where the low rail is less slippery than the high rail. Additionally, for the front axle, the contact condition between the outer wheel and the high rail may also influence the outcome. Typically, a low friction coefficient on curved tracks helps reduce lateral creep forces. As lateral creep forces exert less strength, a smaller rolling radius is required for the outer wheel. A reduced rolling radius leads to an increase in angular velocity. This constitutes another mechanism contributing to the difference in angular velocity observed in the asymmetric friction coefficient conditions for the front axle.

5 Conclusions

In this study, the rotation angular velocity changing of the wheelset on the curved tracks are evaluated. To observe the degrees and tendency of the angular velocity changing, the experiments and simulations are conducted.

By the experiments, these findings are obtained:

- The angular velocity changings of wheelsets on curved tracks are observed by the experiments.
- The degree of the changing differs between the front and rear axles of the bogies: the angular velocity of the front axle is slower than that of the rear axle.

Additionally, the simulation results are indicated:

- The same tendency as the experiments are observed, which suggests that the physical phenomenon of the angular velocity changing can be simulated by the FASTSIM algorithm.
- The changing of the angular velocity is affected by the asymmetric condition of wheel/rail friction coefficient.

The mechanism of the angular velocity is discussed by the formulated factors (influence rates). These consequences are obtained as a mechanism of the different angular velocity between the front and rear axles:

- The effect of the path length difference between wheels and the rolling radius changing of wheels are hardly affected by the axle positions. (Notably, it is possibly unique characteristics of the single-axle steering bogie)
- The directions of the longitudinal creepages are different between the axles; it is considered to the primary cause of the difference of the angular velocity.

Additionally, as that between the asymmetric friction coefficient conditions, these findings are obtained:

- The primary cause of the difference of the angular velocity is the degrees of the longitudinal creepages; The wheelsets rotate more dependently to the higher friction coefficient side of the rail.

When conditions such as the curve radius and the steering characteristics of the bogie are different, the degrees and characteristics of the angular velocity changing possibly differed. It is necessary to examine these effects to the angular velocity changing to deepen this study.

References

[1] Nakashima, K., Yanagida, T., Fujii, K., Oki, S., Lim, S., ”New CBTC System for Smart Operation”, Hitachi Review 67(7), 66-70, 2018.

[2] Shimokawa, Y., Mizuno, M., ”Development of the New Concept Steering Bogie”, Nippon Steel & Sumitomo Metal Technical Report (105), 41-47, 2013.

[3] Endo, Y., Michitsuji, Y., Tanimoto, M., Imahori, O., Shimura, K., ”Study on the mechanism of wheelset rotational velocity variation in curved track”, The Proceedings of The 28th IAVSD International Symposium on Dynamics of Vehicles on Roads and Tracks, No.73, 2023.

[4] Kalker, J. J., ”Three-Dimensional Elastic Bodies in Rolling Contact”, (Editor), Kluwer Academic Publishers, Dordrecht, Netherlands, 2010.

[5] Matsumoto, A., Sato, Y., Ohno, H., Shimizu, M., Kurihara, J., Tomeoka, M., Saitou, T., Michitsuji, Y., Tanimoto, M., Sato, Y., Mizuno, M., ”Continuous observation of wheel/rail contact forces in curved track and theoretical considerations”, Vehicle System Dynamics, Vol.50, 349-364, 2012.

[6] Ichiyanagi, Y., Michitsuji, Y., Matsumoto, A., Sato, Y., Ohno, H., Ogata, S., Tanimoto, M., Fukushima, T., Matsuda, T., Shinagawa, D., ”Simulation-based estimation of wheel/rail friction coefficient and wear number considering results of full-scale roller rig test”, Mechanical Engineering Journal 10(3), 2023.